

1 *Communication*

2 **Comparison of Nano-Mechanical Behavior between** 3 **Selective Laser Melted SKD61 and H13 Tool Steels**

4 **Jaechol Yun^a, Van Luong Nguyen^a, Jungho Choe^a, Dong-yeol Yang^a, Hak-sung Lee^{a,b},**
5 **Sangsun Yang^a, Ji-Hun Yu^{a,*}**

6 ^a Powder & Ceramic Division, Korea Institute of Materials Science (KIMS), Changwon 51508, Korea

7 ^b Materials Processing Innovation Research Division, Korea Institute of Materials Science (KIMS), Changwon
8 51508, Korea

9 * Corresponding author. jhyu01@kims.re.kr; Tel.: +82-55-280-3587, Fax: +82-55-280-3289

10
11

12 **Abstract:** Using nanoindentation under various strain rates, the mechanical properties of a
13 selective laser melted (SLM) SKD61 at the 800 mm/s scan speed was investigated and compared to
14 SLM H13. No obvious pile-up due to the ratio of the residual depth (h_r) and the maximum depth
15 (h_{max}) being lower than 0.7 and no cracking were observed on any of the indenter surfaces. The
16 nanoindentation strain-rate sensitivity (m) of SLM SKD61 was found to be 0.034, with hardness
17 increasing from 8.65 GPa to 9.93 GPa as the strain rate increased between 0.002 s^{-1} and 0.1 s^{-1} . At the
18 same scan speed, the m value of SLM H13 ($m = 0.028$) was lower than that of SLM SKD61, indicating
19 that the mechanical behavior of SLM SKD61 was more critically affected by the strain rate
20 compared to SLM H13. SLM processing for SKD61 therefore shows higher potential for advanced
21 tool design than for H13.

22 **Keywords:** Selective laser melting, SKD61 tool steel, nanoindentation, strain-rate sensitivity.

23

24 **INTRODUCTION**

25 SKD61 and H13 are types of hot work tool steels applied to casting molds, extrusion tools,
26 forging dies, etc., and the hardness of SKD61 (229 BHN) is lower than that of H13 (235 BHN) [1-4].
27 Both steels are fabricated by conventional methods requiring expensive dedicated tools, and thus
28 are inappropriate for small-scale or complex-shape productions [1-3]. Selective laser melting (SLM),
29 is a laser powder-bed additive manufacturing process, that is suitable for processing of tool steels
30 including SKD61 and H13 because it offers the ability to not only reduce the amount of machining
31 and hence wastage of this expensive material, but also to produce intricate molds with a nearly full
32 density and a refined microstructure [2,3].

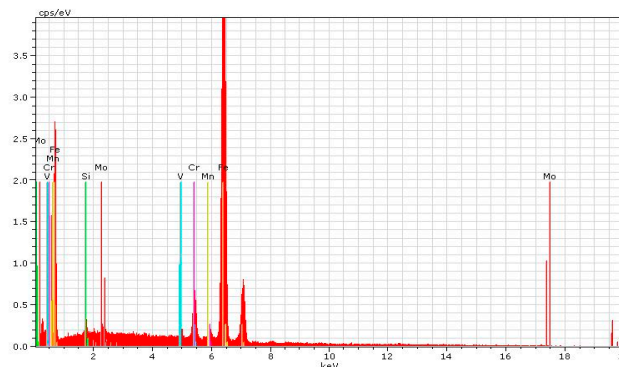
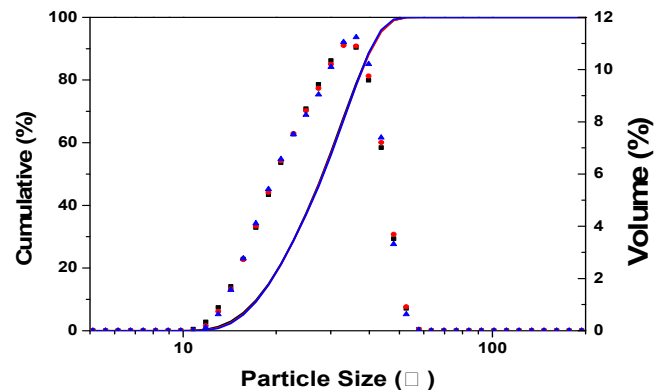
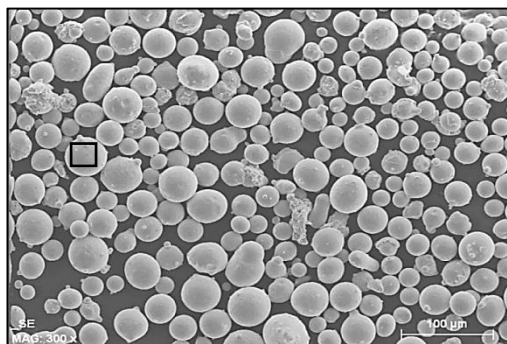
33 The mechanical behavior of hot work tool steels prepared by the SLM method is one of the
34 most important characteristics. It was reported that the hardness of SLM SKD61 fabricated from
35 commercial powders was higher than that made from gas atomized spherical powders [3]. Very
36 recently, a few studies have addressed the mechanical properties of tool steel processed by SLM
37 using nanoindentation [2]. For example, the H13 SLM-ed at 200 mm/s scan speed exhibited the
38 lowest creep resistance and highest hardness values. However, very few studies have dealt with the
39 mechanical behavior of SLM SKD61 using nanoindentation. It is thus necessary to perform

40 nanoindentation tests to probe the creep behavior of the SLM SKD61 and compare it with that of
41 SLM H13.

42 In a previous study, SLM processing at 800 mm/s laser scan speed was applied successful for
43 SKD61 powders [3]. This study expands on that reported findings by using nanoindentation tests to
44 investigate the mechanical properties of SLM SKD61. Results for SLM-processed H13 at the same
45 laser scan speed sourced from the literature are used in the evaluation conducted here [2]. It is
46 demonstrated that nanoindentation strain-rate sensitivity of the SLM SKD61 is more critical to
47 strain rate compared to SLM H13.
48

49 EXPERIMENTAL PROCEDURE

50 The material used in this work was SKD61 powder prepared by a gas atomizing process (Hot
51 Gas Atomization System, HEMMIGA 100/25, PSI Ltd., UK), as shown in Fig. 1. Specifically, SKD61
52 ingot obtained from SeAH Special Steel Corp. (Korea) was melted into a graphite crucible at 1690
53 °C under a high purity argon atmosphere. The alloy liquid was then ejected through a spray nozzle
54 under hot N₂ gas pressure of 50 bar. Upon gas atomization, the gas-atomized powders were
55 collected and loaded onto a series of ASTM E11 standard sieves to obtain a specific particle size
56 range of 10–45 μm. The elemental chemical compositions of the produced powders were confirmed
57 by inductively coupled plasma (ICP, Spectro Arcos ICP-AES, Germany). The powders were then
58 processed by a SLM device (a Concept LaserMlab-Cusing system, Germany) equipped with a 90 W
59 Nb:YAG fiber laser to manufacture cuboid specimens (10 × 10 × 10 mm). Detailed preparation of the
60 SLM samples was described in [2,3].
61



85 Fig. 1. (a) SEM picture of the powder input; (b) particle size distribution; and (c) EDS result at the location
86 indicated by the rectangle in Fig. (a)

87

88 The cuboid specimens prepared by SLM were mounted in epoxy resin, cross-sectioned and then
89 mechanically polished on an auto-disc polishing machine (Struers LaboForce-100, Denmark) to

90 reach mirror-like surfaces. The specimens with a surface roughness of lower than 50 nm determined
 91 using a specialized measuring instrument (Mitutoyo, SV-3200S4, Japan) were used for the next
 92 steps. An optical microscope (OM, Nikon ECLIPSE MA200, Japan) and a scanning electron
 93 microscope (SEM, JSM-5800, JEOL, Japan) were also used to observe the microstructure on the
 94 sample surfaces. Nanoindentation tests were then performed for those samples at room
 95 temperature at the same maximum load (500 mN) on a NanoTest nanoindenter (Micro Materials
 96 Ltd., Wrexham, UK) using a three-sided Berkovich diamond indenter. Specifically, all
 97 nanoindentation tests were carried out at loading rates of 50 mN/s, 25 mN/s, 16.67 mN/s, 12.5 mN/s,
 98 10 mN/s, 5 mN/s and 1 mN/s. The indenter was then held at the maximum load for 5 s, which was
 99 followed by unloading at a rate of 50 mN/s for all tests. At least ten indentation points at each
 100 loading rate were carried out and the results were averaged.

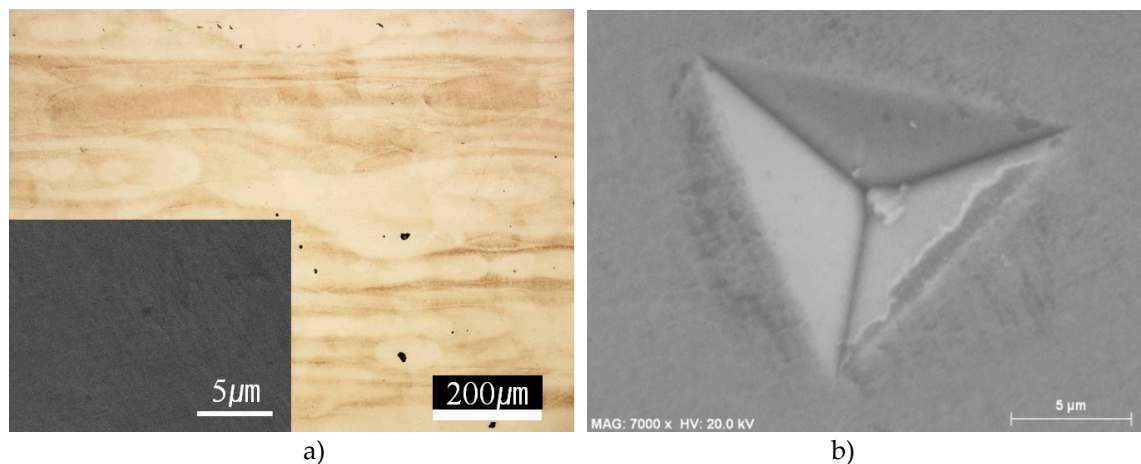
101

102 RESULTS AND DISCUSSION

103 Figure 2a shows a microstructure result of the SKD61 sample prepared by SLM at 800 mm/s
 104 scanning speed, in where the inset is the SEM result. Fig. 1b shows a SEM result at the location of an
 105 indenter point. Fig. 2a reveals some black pores with irregular shapes and small volumes observed
 106 over the sample. The volume fraction of the black phase was calculated using the image analysis
 107 software to be 1.4%, which is lower than that (5.2%) for SLM H13 at the same scan speed [2]. Black
 108 pores, indicating imperfections in the microstructure, may stem from insufficient laser energy to
 109 melt powder materials within the melt pool, causing a short cooling (faster solidification) time and
 110 insufficient melting of the substrate and powders [2].

111

112



113

114

115

116

117

Fig. 2. (a) Microstructure of the SLM- processed SKD61 at 800 mm/s scanning speed; (b) SEM graph of an indenter point after nanoindentation tests

118

119

120

121

122

123

124

125

126

127

128

The widely used Oliver and Pharr method is accurate only for nanoindentations that do not show significant pile-up deformation, which is related to the ratio of the residual depth (h_f) and the maximum depth (h_{max}) [5]. In the SEM results of indenter points on all sample surfaces, no obvious pile-up is observed, as shown in Fig. 1b. This result is similar to that of SLM H13 material, where it was confirmed that $\frac{h_f}{h_{max}}$ in all nanoindentation tests was lower than 0.7 [2]. Therefore, the Oliver and Pharr method can be adopted to extract the hardness values of the material here. Moreover, no cracking in Fig. 1b is observed, indicating that the material has low crack sensitivity.

In this study, a constant rate of loading (CRL) method, where a steady loading rate is used until the tip depth rate becomes nearly constant, is used to determine the strain rate ($\dot{\epsilon}$) because the CRL allows for simple calculation of strain rates, and also is proven to be more suitable to correlate with the conventional constant strain rate tests [6]. In fact, both indentation hardness and strain rate are

129 not constant under CRL loading, causing difficulty in determining of a consistent creep exponent
 130 from a single CRL nanoindentation experiment [6]. However, if only the indentation hardness and
 131 indentation strain rate at the maximum load point are used, the strain-rate sensitivity can be
 132 determined from a group of CRL nanoindentation tests under different loading rates [6].
 133 Accordingly, the above loading rates correspond to strain rates of 0.1 s^{-1} , 0.05 s^{-1} , 0.033 s^{-1} , 0.025 s^{-1} ,
 134 0.02 s^{-1} , 0.01 s^{-1} , and 0.002 s^{-1} , respectively.

135 Figure 3 is plotted to compare the hardness of SKD61 and H13 processed by SLM at 800 mm/s
 136 scan speed. Error bars on the data reflect the standard deviation calculated for hardness from
 137 multiple indentations for each sample. Experimental results from nanoindentation tests of H13
 138 prepared by SLM at 800 mm/s, obtained from another report in the literature, are included for
 139 comparison [2]. As shown in Table 1, the hardness increases in ranges of (8.65–9.99) GPa and (7.91–
 140 8.84) GPa for the SKD61 and H13 materials, respectively, prepared by SLM at the same scan speed
 141 of 800 mm/s at nanoindentation strain rates in the range of 0.002 s^{-1} and 0.1 s^{-1} . This shows the SLM
 142 SKD61 has about 10% higher hardness values on average than the SLM H13 material.

143

144 *Table 1. Hardness values of SKD61 and H13 prepared by the SLM process at the same scan speed of 800*

145

Strain rate (s^{-1})	mm/s	
	Hardness (GPa)	
	SKD61	H13 [2]
0.002	8.65	7.91
0.01	9.26	8.16
0.02	9.43	8.41
0.025	9.26	8.32
0.033	9.55	8.53
0.05	9.70	8.61
0.1	9.93	8.84

146

147 By assuming the indentation strain rate and hardness are proportional to the flow strain rate
 148 and stress, respectively, it follows that the strain rate sensitivity (SRS) can be defined as

149

$$m = \left(\frac{\partial \ln H}{\partial \ln \dot{\epsilon}} \right), \quad (1)$$

150

The slope of the straight line in Fig. 3 represents the strain-rate sensitivity exponent (m), with a
 151 value of 0.034 and 0.028 for the SLM SKD61 and H13, respectively. The strain-rate sensitivity of
 152 SLM SKD61 is higher than that of SLM H13, indicating that the mechanical behavior of H13
 153 material is less susceptible to the strain rate than SKD61.

154

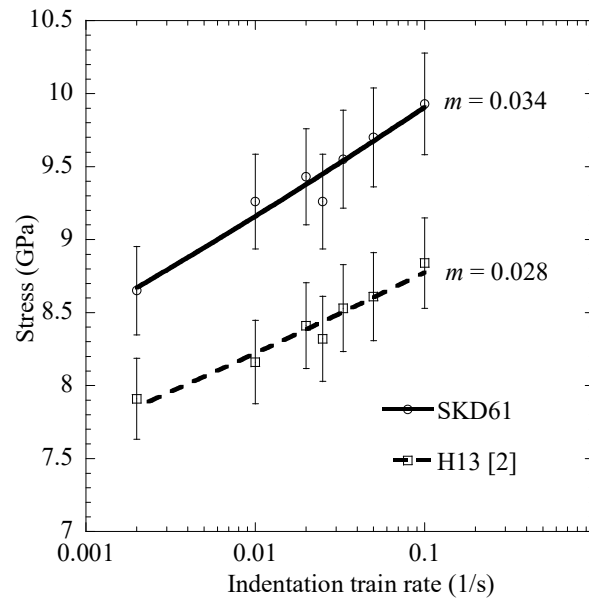


Fig. 3. Indentation stress as a function of strain rate for SLM-processed by SKD61 and H13

155

156

157

158

159

160

161

162

163

164

165

166 CONCLUSION

167

168

169

170

171

172

173

174

175

176

177

178

179

180

181

182

In recent studies, the optimal laser scan speed for the SLM process is around 200 mm/s for H13 [2], and the hardness increased from 8.61 GPa to 9.29 GPa, and these values are lower than those of SKD61 in the present study at the same strain rate range. Because the laser energy density is inversely proportional to the scan speed [7], the optimal condition of the SLM process for SKD61 consumes less energy than for H13. Moreover, SLM SKD61 shows better microstructure (less pores) and higher hardness than SLM H13. Therefore, SLM SKD61 shows higher potential for advanced tool design than SLM H13.

This study demonstrates successful printing of SKD61 by the SLM method at 800 mm/s laser speed. From the results, no obvious pile-up (due to $\frac{h_f}{h_{max}} < 0.7$) and no cracking on all indenter surfaces were observed. Hardness increased from 8.65 GPa to 9.93 GPa as the strain rate increased in a range of 0.002 s⁻¹ and 0.1 s⁻¹. At the same scan laser speed, the m value of SLM SKD61 ($m = 0.034$) is higher than that of SLM H13 ($m = 0.028$), indicating that the mechanical behavior of the SLM SKD61 was more critical to the strain rate compared to SLM H13. As a result, SLM processing for SKD61 shows higher potential in practical application than for H13 due to the superior microstructure and mechanical behavior of the former, and less laser energy consumption at the optimal condition.

ACKNOWLEDGEMENTS: This study was supported financially by the Fundamental Research Program of the Korean Institute of Materials Science (KIMS).

177 REFERENCES

1. Sander, J.; Hufenbach, J.; Giebler, L.; Wendrock, H.; Kuhn, U.; Eckert, J. Microstructure and properties of FeCrMoVC tool steel produced by selective laser melting. *Mater. Des.* **2016**, *89*, 335–341.
2. Nguyen, V.L; Kim, E.A.; Lee, S.R.; Yun, J.C.; Choe, J.H.; Yang, D.Y.; Lee, H.S.; Lee, C.W.; Yu, J.H. Evaluation of strain-rate sensitivity of selective laser melted H13 tool steel using

- 183 nanoindentation tests. *Metals* **2018**, *8*, 589.
- 184 3. Yu, J.H.; Yang, D.Y.; Lee, H.S.; Kim, S.W.; Yang, S.S.; Lim, T.S.; Lee, C.W. Characteristics of
185 SLM printed SKD61 alloy by using of gas atomized spherical powders. *KSME Spring Conf.* **2016**,
186 1143–1144.
- 187 4. <http://www.astmsteel.com/steel-knowledge/hot-work-steel-h13-1-2344-sk61/>
- 188 5. Oliver, W.C.; Pharr, G.M. An improved technique for determining hardness and elastic
189 modulus using load and displacement sensing indentation experiments, *J. Mater. Res.* **1992**, *7*,
190 1564–1583.
- 191 6. Du, Y.; Liu, X.H.; Fu, B.; Shaw, T.M.; Lu, M.; Wassick, T.A.; Bonilla, G.; Lu, H. Creep
192 characterization of solder bumps using nanoindentation. *Mech. Time-Depend Mater.* **2017**, *21*,
193 287–305.
- 194 7. Simchi, A. Direct laser sintering of metal powders: Mechanism, kinetics and microstructural
195 features. *Mater. Sci. Eng. A* **2006**, *428*, 148–158.